ACS APPLIED MATERIALS & INTERFACES

Research Article

www.acsami.org

Graphene-Based Nanocomposite As an Effective, Multifunctional, and Recyclable Antibacterial Agent

Tengfei Tian,[†] Xiaoze Shi,[†] Liang Cheng,[†] Yinchan Luo,[†] Ziliang Dong,[†] Hua Gong,[†] Ligeng Xu,[†] Zengtao Zhong,[‡] Rui Peng,*[,†] and Zhuang Liu*[,†]

[†]Jiangsu Key Laboratory for Carbon-Based Functional Materials and Devices, Institute of Functional Nano & Soft Materials (FUNSOM), Collaborative Innovation Center of Suzhou Nano Science and Technology, Soochow University, Suzhou, Jiangsu 215123, China

[‡]Department of Microbiology, Nanjing Agricultural University, Nanjing, Jiangsu 210095, China

Supporting Information

ABSTRACT: The development of new antibacterial agents that are highly effective are of great interest. Herein, we present a recyclable and synergistic nanocomposite by growing both iron oxide nanoparticles (IONPs) and silver nanoparticles (AgNPs) on the surface of graphene oxide (GO), obtaining GO-IONP-Ag nanocomposite as a novel multifunctional antibacterial material. Compared with AgNPs, which have been widely used as antibacterial agents, our GO-IONP-Ag shows much higher antibacterial efficiency toward both Gram-negative bacteria *Escherichia coli* (*E. coli*) and Gram-positive bacteria *Staphylococcus aureus* (*S. aureus*). Taking the advantage of its strong near-infrared (NIR) absorbance, photothermal treatment is also conducted with GO-IONP-Ag, achieving a remarkable synergistic antibacterial effect to inhibit *S. aureus* at a rather low concentration of this agent. Moreover, with magnetic IONPs existing in the composite, we can easily recycle GO-IONP-Ag by magnetic separation, allowing its repeated use. Given the above advantages as well as its easy preparation and cheap cost, GO-IONP-Ag developed in this work may find potential applications as a useful antibacterial agent in the areas of healthcare and environmental engineering.

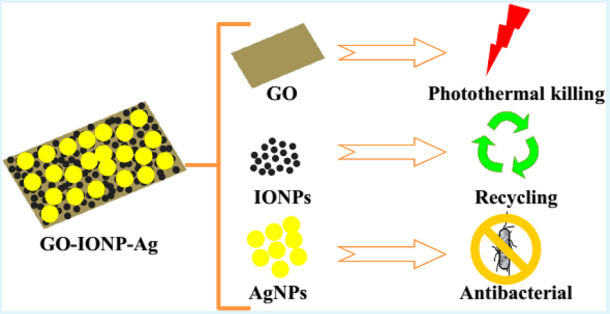

KEYWORDS: *graphene nanocomposite, antibacterial, synergistic effect, photothermal, recycling*

INTRODUCTION

Antimicrobial resistance is a global concern as it makes the antibiotics largely useless and significantly increases the cost of healthcare.[1−3] New generations of antimicrobials that can effectively kill pathogenic bacteria are thus urgently needed. In recent years, a large number of nanomaterial-based antimicrobials have been developed.[4] Among them, AgNPs and silver-based antimicrobials are the most widely explored and used nano-agents owing to their great antimicrobial activity, broad antimicrobial spectrum and low propensity to induce bacteria resistance.[5−9] In addition, in order to reduce the cost of antimicrobials, especially when they are used in large scales (e.g. to treat contaminated water sources), those agents should be easily separated, and more ideally, recyclable.[10−12]

Graphene and graphene-based nanocomposites have also been used in bacteria detection and antibacterial applications.[13−31] It has been reported that GO presents antibacterial effect, although the mechanisms and efficacies are under certain debate.[14,31−34] In addition, AgNPs anchored GO (GO-Ag) have been synthesized by different groups for antimicrobial applications.[16−20,22,25,27−29] In our recent study, we found that GO-Ag nanocomposite showed markedly enhanced antibacterial effects compared to bare AgNPs.[15] Moreover, with strong optical absorbance in the near-infrared (NIR) region, graphene could be used as a photothermal agent not only to ablate tumors in cancer treatment,[35−42] but also to effectively kill bacteria.[43−47] Despite those encouraging findings, the use of graphene-based nanocomposite to kill bacteria in a recyclable and synergistic manner remains to be further explored.

In this work, by growing IONPs and AgNPs on the surface of GO, a new type of antibacterial agent, namely GO-IONP-Ag nanocomposite, is obtained. Because of the enhanced antibacterial property of GO-IONP-Ag, not only Gram-negative bacteria *E. coli* but also Gram-positive bacteria *S. aureus* are greatly inhibited by this agent, which appears to be much more effective than bare AgNPs. The photothermal effect of GO-IONP-Ag is then utilized to further enhance its antibacterial ability, allowing effective killing of *S. aureus* under a rather low concentration after laser exposure. Last but not the least, we further demonstrate that our GO-IONP-Ag can be easily separated by magnetic attraction and used in a recyclable manner. Thus, our study presents a multifunctional

Received: March 8, 2014
Accepted: May 7, 2014
Published: May 7, 2014

   dx.doi.org/10.1021/am5022914 | ACS Appl. Mater. Interfaces 2014, 6, 8542−8548

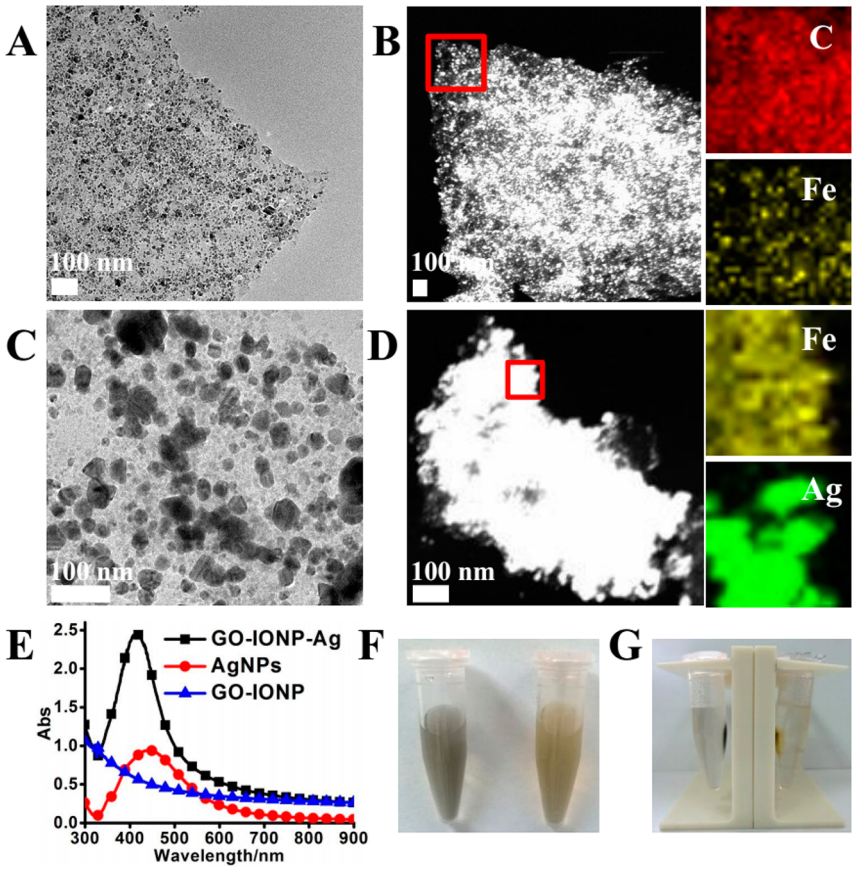

Figure 1. Characterization of GO-IONP and GO-IONP-Ag. (A) TEM image of GO-IONP. (B) STEM image of GO-IONP and the corresponding HAADF-STEM-EDS mapping images showing carbon edge (red) and iron edge (yellow) in the selected area (red rectangle). (C) TEM image of GO-IONP-Ag. (D) STEM image of GO-IONP-Ag and the corresponding HAADF-STEM-EDS mapping images showing iron edge (yellow) and silver edge (green) in the selected area (red rectangle). (E) UV–vis absorbance spectra of AgNPs, GO-IONP, and GO-IONP-Ag dispersed in water. (F, G) Photographs of GO-IONP solution (left) and GO-IONP-Ag solution (right) in water in the (F) absence and (G) presence of external magnetic field.

graphene-based nanocomposite as an effective, multifunctional, and recyclable antibacterial agent.

EXPERIMENTAL SECTION

Synthesis and Characterization of GO-IONP-Ag Nanocomposite. Following to a previously reported protocol, IONPs anchored GO (GO-IONP) was synthesized first.[35,48] For the further growth of AgNPs, 4 mL of GO-IONP solution (1.42 mg/mL by GO) was mixed with 18 mg of silver nitrate dissolved in 100 mL of deionized (DI) water under stirring in oil bath. Sodium citrate (20 mg) was then added into the boiling aqueous solution, which was further boiled for 1 h. The synthesized nanocomposite was purified by centrifugation and washing with DI water.

Silver nanoparticles were synthesized by a previously established method.[49] Briefly, 20 mg of sodium citrate was added into 100 mL of boiling DI water containing 18 mg of silver nitrate. The mixture was kept boiling for 1 h to yield AgNPs.

The contents of silver and iron in the obtained GO-IONP-Ag nanocomposite were measured by inductively coupled plasma atomic emission spectroscopy (ICP-AES) after it was decomposed with nitric acid. Transmission electron microscopy (TEM) and elemental mapping in the high-angle annular dark-field scanning transmission electron microscopy (HAADF-STEM) images of GO-IONP and GO-IONP-Ag were taken using transmission electron microscopy (Tecnai G20 F20, FEI).

Bacteria Culture and Antibacterial Studies. A single colony was isolated from the Luria-Bertani (LB) agar plate, added into fresh LB broth for incubation at 37 °C within a shaking incubator at speed of 255 rounds-per-minute (RPM) overnight, and then diluted 100 times for bacteria growth into log phase before usage.

The concentrations of viable bacteria were measured by colony formation unit (CFU) counting. Log phase growth bacteria were adjusted to about 1×10^7 to 1×10^8 CFU/mL with fresh LB broth. Different materials were added into the bacteria suspension at the volume of 1/10 of bacterial suspension, which was then incubated in the shaking incubator at 37 °C at the speed of 255 rpm for 2.5 h. At the end of incubation, 100 μL of diluted bacteria suspension was dispersed in 96-well plate and co-incubated with 20 μL of 3-(4, 5-dimethylthiazol-2-yl)-2, 5-diphenyl tetrazolium bromide (MTT). The formed precipitates were dissolved in dimethyl sulfoxide (DMSO) for analyzing using a microplate reader (Bio-Rad). All the measurements were carried out for at least three times. Two bacteria species were used here: Gram-positive bacteria *S. aureus* (a gift from clinical laboratory in the First Affiliated Hospital of Soochow University) and Gram-negative bacteria *E. coli* DH5α.

Minimum Inhibitory Concentration (MIC) Determination. MIC values of bacteria were determined according to the standard protocol.[50] In brief, 2 μL of 1×10^4 CFU bacteria were delivered onto the surface of agar plates containing serial dilutions of antibiotics or GO-IONP-Ag nanocomposite at final concentrations from 1 to 512 mg/L (silver content for GO-IONP-Ag). Then, the agar plates were incubated in 37 °C incubator for 20 h. The MIC values are defined as the lowest concentration of antibiotics or nanocomposite at which there was no visible bacterial growth.

Photothermal Killing of *S. aureus*. Photothermal heating curves were obtained with an infrared thermal camera to monitor the temperature change during the laser irradiation (808 nm, 1.5 W/cm^2, 7

dx.doi.org/10.1021/am5022914 | ACS Appl. Mater. Interfaces 2014, 6, 8542–8548

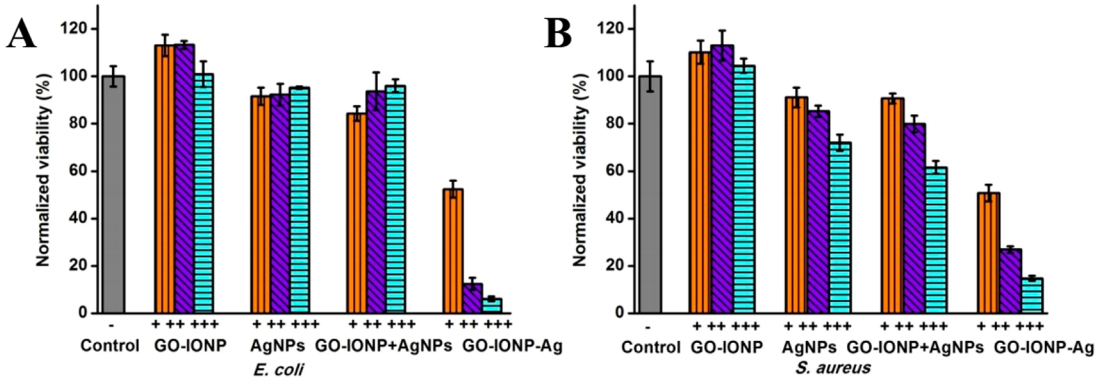

Figure 2. Cell viabilities of (A) *E. coli* and (B) *S. aureus* after treatment with GO-IONP, AgNPs, a simple mixture of GO-IONP and AgNPs, as well as GO-IONP-Ag nanocomposite at different concentrations for 2.5 h. Symbols +, ++, and +++ represent final concentrations of silver at 2 μg/mL (+), 4 μg/mL (++), and 8 μg/mL (+++) respectively, and the corresponding GO-IONP concentrations at 1.6 μg/mL (+), 3.2 μg/mL (++), and 6.4 μg/mL (+++), respectively. Error bars represent the standard deviations ($n \geq 3$).

min) in real time. AgNPs, GO-IONP, and GO-IONP-Ag were dissolved in LB broth at the same corresponding final concentration at [Ag] = 4 μg/mL and [GO-IONP] = 3.2 μg/mL.

Photothermal efficiency of nanomaterials was determined by the MTT assay and spread plate method. At first, 100 μL water, GO-IONP and GO-IONP-Ag aqueous solutions were incubated with 900 μL of *S. aureus* (1×10^7 to 1×10^8 CFU/mL) for half an hour, and the bacteria suspension was then exposed to laser irradiation (808 nm) at different power densities (0, 1, 1.5, and 2 W/cm^2) for 7 min with three parallel samples for each group. Then, the irradiated samples were re-incubated in the shaking incubator at 37 °C for 5.5 h. At last, appropriate volume of bacterial suspension was diluted and incubated with 20 μL of 5 mg/mL MTT before reading the number of viable bacteria by the microplate reader (Bio-Rad). Spread plate method was also used to count the viable colonies. In this case, 40 μL of diluted bacteria were spread on the agar plate, and then the plates were placed in a 37 °C incubator for 14 h.

Recycling of GO-IONP-Ag Nanocomposite. Two hundred microliters of GO-IONP-Ag was added into 1.8 mL of *E. coli* suspension to a final concentration of 50 μg/mL (silver content). The cell suspension was then incubated in a 37 °C shaking incubator for 2.5 h. A small volume of cell suspension was taken for MTT assay to determinate the relative cell viability. The leftover suspension was put on a magnetic shelf to separate the magnetic nanocomposite. The separated GO-IONP-Ag nanocomposite was washed once and then used for the next round of antibacterial application.

RESULTS AND DISCUSSION

The GO-IONP-Ag nanocomposite was synthesized by a two-step process. Following our previously reported protocol, we firstly prepared magnetic GO-IONP composite,[35] on to which AgNPs were grown. The synthesized GO-IONP and GO-IONP-Ag were soluble in aqueous solution without the need of further modification. TEM and elemental mapping in HAADF-STEM imaging were employed to characterize the obtained composite nanomaterials (Figure 1A–D). For the GO-IONP sample, many small nanoparticles were anchored on GO sheets homogeneously. Further elemental mapping in HAADF-STEM imaging confirmed that Fe_3O_4 nanoparticles (yellow color, iron) were successfully deposited on the graphene (red color, carbon) sheet (Figure 1B). On the second step, AgNPs with larger sizes were anchored on GO-IONP sheets (Figure 1C). Compared with GO-IONP, the AgNP-anchored GO-IONP sheets appeared to be much brighter in the dark field. HAADF-STEM imaging of the random selected area (red box) indicated large amount of silver (green color) formed on those nanosheets (Figure 1D). Note that we used the Ag content to present the concentrations of GO-IONP-Ag nanocomposite in our following studies.

UV–vis absorbance spectra of AgNPs, GO-IONP, and GO-IONP-Ag were then recorded (Figure 1E). A strong AgNP characteristic absorbance peak at 410 nm was observed for both AgNPs and GO-IONP-Ag samples, suggesting the existence of AgNPs in the obtained nanocomposite. Different from AgNPs, both GO-IONP and GO-IONP-Ag showed strong absorbance at longer wavelength (e.g., the NIR region), which was attributed to the optical absorbance of GO. Correspondingly, the aqueous solution of GO-IONP-Ag turned into yellowish after silver deposition on GO-IONP (Figure 1F). Moreover, with the maintained magnetic property, the synthesized GO-IONP-Ag could be easily adsorbed by a magnet placed nearby, leaving with limpid water in the tube (Figure 1G). Therefore, we use the Ag content in the GO-IONP-Ag for antibacterial application, the NIR absorbance contributed from GO for photothermal killing of bacteria, and the magnetic property originated from IONPs for magnetic separation and recycling of materials.

Gram-negative bacteria *E. coli* and Gram-positive bacteria *S. aureus* were then selected as the model organisms to evaluate the antibacterial efficiency of GO-IONP-Ag. Bacteria suspensions with an initial concentration of 1×10^7 to 1×10^8 CFU/mL, which was rather high compared to that used in many previously reported studies,[16,31,46,51–53] were used in our experiments. An incubation time of 2.5 h was chosen to make sure that the bacteria were in the middle of their log growth phase, which was important to study the realistic antimicrobial efficiency of antimicrobials. As shown in Figure 2, compared with AgNPs treated group, the viabilities of *E. coli* and *S. aureus* decreased obviously as the concentration of GO-IONP-Ag increased. At the final concentration of 8 μg/mL (silver content, +++) in GO-IONP-Ag treated bacteria suspension, the remained relative viabilities of *E. coli* and *S. aureus* were 6.1 and 14.7%, whereas those in the AgNPs treated group (at the same silver concentration) were 95.2 and 72%, respectively (Figure 2). The MIC values of GO-IONP-Ag were also found to be remarkably lower than those of bare AgNPs for both types of bacteria (Table 1 and Figure S3 in the Supporting Information). In control experiments, on the other hand, GO-IONP did not contribute to the growth inhibition of bacteria, and the mixture of AgNPs and GO-IONP had no obvious additional inhibitory effect on *E. coli* and *S. aureus*.

dx.doi.org/10.1021/am5022914 | ACS Appl. Mater. Interfaces 2014, 6, 8542–8548

Table 1. MIC Values of Various Agents Towards Both Gram-Negative and Gram-Positive Bacteria

bacteria	GO-IONP-Ag (mg/L)	ampicillin (mg/L)	AgNPs (mg/L)
S. aureus	8 (Ag), 14.4 (GO-IONP-Ag)	<1	32
E. coli	8 (Ag), 14.4 (GO-IONP-Ag)	16	32

The unique synergistic antibacterial effects may be attributed to the existence of 2D GO sheet in the nanocomposite. As proposed in previous studies,[15,28] GO sheets with hydrophobic domains in the nanocomposites may allow effective attachment of nanomaterials on the surface of bacteria, thus increasing the contact between AgNPs decorated on GO and the bacteria. Moreover, as the supporter of AgNPs, GO sheets could prevent the aggregation of AgNPs and protect their high surface reactivity. As a result, AgNP-loaded GO-based nanocomposite, such as GO-IONP-Ag developed in our work, shows synergistic enhancement in terms of antibacterial efficiency in comparison to bare AgNPs.

In order to understand the bacteria-type-dependent antibacterial mechanism of GO-IONP-Ag, scanning electron microscope (SEM) images of treated *E. coli* and *S. aureus* were taken (see Figure S1 in the Supporting Information). For *E. coli*, in contrast with normal smooth rod-shaped bacteria shown in the control group (see Figure S1A in the Supporting Information), many pits (red arrow) were found for GO-IONP-Ag treated bacteria (Figure S1B), indicating that the integrity of bacteria was damaged.[6,54] As a result, the remained cell viabilities dropped dramatically as the increase of GO-IONP-Ag concentrations (Figure 2A). On the contrary, the integrity of *S. aureus* was rarely damaged but their surfaces became rough and were covered by nanomaterials (see Figure S1D in the Supporting Information), which corresponded to our hypothesis. A further time-lapse observation was done under optical microscope (see Figure S2 in the Supporting Information). Almost every bacterium in control group divided once within 90 min of observation (see Figure S2A in the Supporting Information), whereas no bacterium division was found in the GO-IONP-Ag treated group (see Figure S2B in the Supporting Information). Therefore, while Gram-negative *E. coli* are killed by GO-IONP-Ag likely as a result of cell wall/membrane damage, and Gram positive *S. aureus*, which have multilayer positively charged peptidoglycan on their surface,[15,55] are not directly damaged by our nano-agent. Instead,

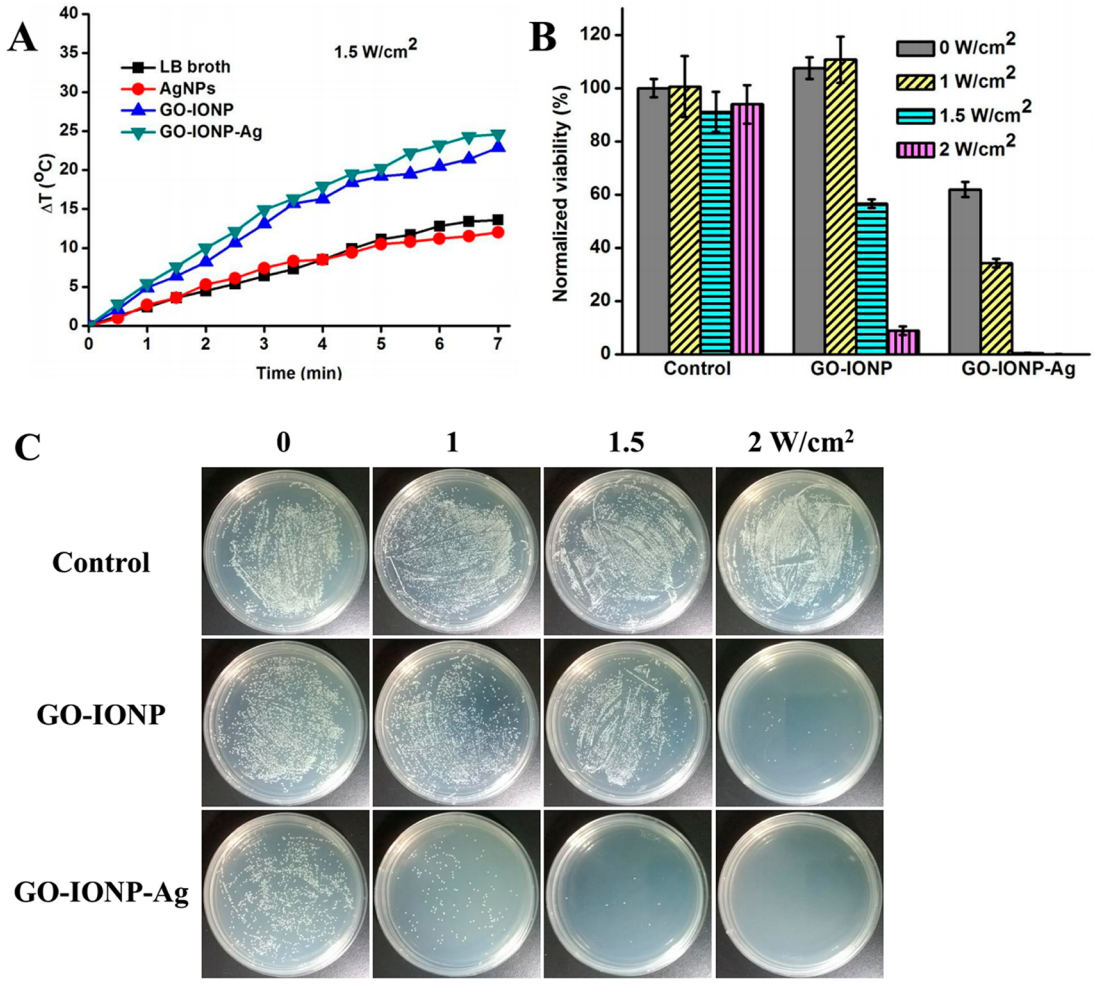

Figure 3. Photothermal treatment of *S. aureus*. (A) Photothermal heating curves of LB broth, AgNPs (4 μg/mL), GO-IONP (3.2 μg/mL), and GO-IONP-Ag ([Ag] = 4 μg/mL, [GO-IONP] = 3.2 μg/mL) under laser irradiation (808 nm, 1.5 W/cm^2, 7 min). (B) Remaining viabilities of GO-IONP and GO-IONP-Ag treated *S. aureus* bacteria after laser irradiation at different power densities (0, 1, 1.5, and 2 W/cm^2) for 7 min. Error bars represent the standard deviations ($n \geq 3$). (C) Photographs of *S. aureus* colonies grew on LB agar plates after incubation with GO-IONP or GO-IONP-Ag and then exposure to the 808 nm laser at different power densities.

dx.doi.org/10.1021/am5022914 | ACS Appl. Mater. Interfaces 2014, 6, 8542−8548

their cell division could be greatly inhibited after GO-IONP-Ag treatment (Figure 2B).

As revealed by the above data, when the concentration of GO-IONP-Ag was 4 μg/mL (silver content, 7.2 μg/mL for entire composite) in bacteria suspension, a concentration below its MIC, the growth inhibitory effect was limited for *S. aureus* (remained viability = 61.9% ± 2.9%) (Figure 3B). We thus wondered whether the photothermal effect of GO-IONP-Ag could be utilized to enhance its bacteria killing ability.[35−37] The bacteria suspension was incubated with GO-IONP-Ag for half an hour and then exposed to an 808 nm laser at different power densities for 7 min. MTT assay was then conducted after further incubation for 5.5 h in order to determine whether the bacteria growth was completely inhibited. As shown in Figure 3A, rapid temperature rises were observed for LB broth containing GO-IONP and GO-IONP-Ag samples under laser irradiation (1.5 W/cm^2, 7 min), whereas much less effective photothermal heating was noted for LB broth with AgNPs. Correspondingly, no decrease of bacteria viability was observed in the control groups treated with laser irradiation ranged from 0 W/cm^2 to 2 W/cm^2 (Figure 3B). In contrast, the remained viabilities of bacteria treated with GO-IONP-Ag ([Ag] = 4 μg/mL, 7.2 μg/mL for entire nanocomposite) decreased significantly as the increase of laser power densities (Figure 3B), and were almost completely killed under laser irradiation at 1.5 W/cm^2 (remained viability = 0.4% ± 0.1%). The pure photothermal effect offered by GO-IONP, on the other hand, was effective in killing bacteria only under the highest power density at 2.0 W/cm^2 (remained viability = 8.8% ± 1.6%).

To further confirm the photothermally enhanced antibacterial efficacy of GO-IONP-Ag, we used the universal adopted spread plate method to count the viable colonies after various treatments. As shown in Figure 3C, many viable colonies in the untreated group were visible on the LB agar plate after overnight culture in 37 °C incubator. Consistent to the previous MTT data, while laser irradiation by itself was not able to inhibit bacterial growth, photothermal heating induced by GO-IONP could kill bacteria but only at the highest laser power density (2.0 W/cm^2). Again, GO-IONP-Ag treatment plus photothermal heating induced by laser irradiation showed an obvious synergistic antibacterial effect, which appeared to be much more significant than that offered by GO-IONP-Ag without laser exposure. This combined strategy can not only improve the efficiency of nano-agent, but also broaden antibacterial spectrum because not all the bacteria are sensitive enough to AgNPs.

Recyclable antibacterial nanomaterials are eco-friendly as they can reduce the emission of pollutants, usage of raw materials, and cut down the total cost of use. Because of the existence of magnetic IONPs, our GO-IONP-Ag nanocomposite could be easily separated from its aqueous dispersion by applying an external magnetic field. We thus wondered if GO-IONP-Ag could be used as a recyclable antibacterial material. The recycling process is shown in Figure 4A. *E. coli* DH5α was used as the model bacteria for the recycling experiment. Log phase growth bacteria were incubated with GO-IONP-Ag ([Ag] = 50 μg/mL) for 2.5 h. With the help of a magnet, GO-IONP-Ag nanocomposite was separated from the bacteria suspension, which was taken for MTT assay to determine the relative bacterial viability. The leftover nanocomposite was washed to remove the adsorbed protein during the incubation with LB broth, and then dispersed in deionized water for the next cycle of antibacterial application. Different

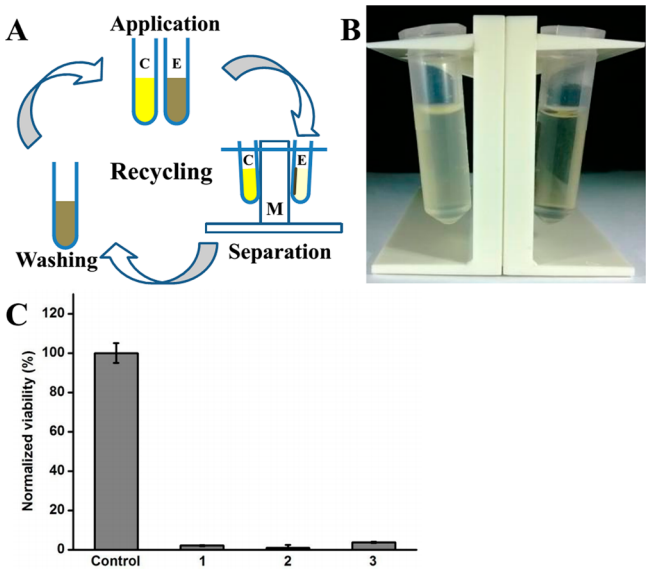

Figure 4. Recyclable antibacterial use of GO-IONP-Ag nanocomposite. (A) Schematic illustration of using GO-IONP-Ag nanoparticles for recyclable antibacterial application. C, untreated bacterial suspension as the control; E, GO-IONP-Ag treated bacteria suspension as the experimental group; M, magnet. (B) Photo showing separation of GO-IONP-Ag in the bacteria suspension. In contrast with control bacteria suspension (left), GO-IONP-Ag treated bacteria suspension (right) was limpid. (C) Relative cell viabilities of GO-IONP-Ag treated bacteria after being repeatedly used for different cycles. Error bars represent the standard deviations ($n \geq 3$).

from the control untreated sample, which appeared as a turbid suspension, the GO-IONP-Ag treated bacteria sample was transparent after magnetic separation, indicating the majority of bacteria were effective killed (Figure 4B). MTT assay revealed that the GO-IONP-Ag agent remained highly effective after being recycled for at least three times (Figure 4C). Compared with previously reported antibacterial agent recycling studies,[10−12,56] we achieved excellent antibacterial efficiency using much less antibacterial agent.

CONCLUSION

In this study, we have synthesized iron oxide and silver co-deposited GO-IONP-Ag nanocomposite, which shows good stability in aqueous solution without any further modification. Compared with pure AgNPs, GO-IONP-Ag offers greatly enhanced antibacterial efficiency toward both Gram-negative bacteria *E. coli* and Gram-positive bacteria *S. aureus*. Taking advantage of the light absorber, GO, in the nanostructure, efficient photothermal killing with GO-IONP-Ag is achieved towards *S. aureus* at a rather low agent concentration. In addition, such GO-IONP-Ag nanocomposite could be easily recycled by magnetic separation, ideally for its further use in an economic and eco-friendly manner. With those unique advantages, the GO-IONP-Ag nanocomposite developed in this work may find potential applications as a multifunctional antibacterial agent in many different fields from healthcare to environmental remediation.

ASSOCIATED CONTENT

Supporting Information

Additional data about SEM images of GO-IONP-Ag treated bacteria, time-lapse photography of bacterial growth, and

dx.doi.org/10.1021/am5022914 | ACS Appl. Mater. Interfaces 2014, 6, 8542−8548

photographs of the MIC assay for various bacteria. This material is available free of charge via the Internet at http://pubs.acs.org.

AUTHOR INFORMATION

Corresponding Authors

*E-mail: rpeng@suda.edu.cn
*E-mail: zliu@suda.edu.cn

Notes

The authors declare no competing financial interest.

ACKNOWLEDGMENTS

This work is supported by the National Basic Research Program (973 Program) of China (2012CB932600, 2011CB911000), the National Natural Science Foundation of China (51222203, 31300824, 51302180, 81371763), China Postdoctoral Science Foundation (2013M530267, 2013M531400), and a Project Funded by the Priority Academic Program Development of Jiangsu Higher Education Institutions.

REFERENCES

(1) Cohen, M. L. Epidemiology of Drug Resistance: Implications for a Post—Antimicrobial Era. *Science* **1992**, *257*, 1050−1055.

(2) Chen, S.; Wang, H.; Katzianer, D. S.; Zhong, Z.; Zhu, J. Lysr Family Activator-Regulated Major Facilitator Superfamily Transporters Are Involved in *Vibrio cholerae* Antimicrobial Compound Resistance and Intestinal Colonisation. *Int. J. Antimicrob. Agents* **2013**, *41*, 188−192.

(3) Zhong, Z.; Yu, X.; Zhu, J. Red Bayberry Extract Inhibits Growth and Virulence Gene Expression of the Human Pathogen Vibrio Cholerae. *J. Antimicrob. Chemother.* **2008**, *61*, 753−754.

(4) Dastjerdi, R.; Montazer, M. A Review on the Application of Inorganic Nano-Structured Materials in the Modification of Textiles: Focus on Anti-Microbial Properties. *Colloids Surf., B* **2010**, *79*, 5−18.

(5) Rai, M.; Yadav, A.; Gade, A. Silver Nanoparticles as a New Generation of Antimicrobials. *Biotechnol. Adv.* **2009**, *27*, 76−83.

(6) Sondi, I.; Salopek-Sondi, B. Silver Nanoparticles as Antimicrobial Agent: A Case Study on *E. coli* as a Model for Gram-Negative Bacteria. *J. Colloid Interface Sci.* **2004**, *275*, 177−182.

(7) Balogh, L.; Swanson, D. R.; Tomalia, D. A.; Hagnauer, G. L.; McManus, A. T. Dendrimer-Silver Complexes and Nanocomposites as Antimicrobial Agents. *Nano Lett.* **2001**, *1*, 18−21.

(8) Kumar, A.; Vemula, P. K.; Ajayan, P. M.; John, G. Silver-Nanoparticle-Embedded Antimicrobial Paints Based on Vegetable Oil. *Nat. Mater.* **2008**, *7*, 236−241.

(9) Randall, C. P.; Oyama, L. B.; Bostock, J. M.; Chopra, I.; O'Neill, A. J. The Silver Cation (Ag^+): Antistaphylococcal Activity, Mode of Action and Resistance Studies. *J. Antimicrob. Chemother.* **2013**, *68*, 131−138.

(10) Dong, A.; Sun, Y.; Lan, S.; Wang, Q.; Cai, Q.; Qi, X. Z.; Zhang, Y. L.; Gao, G.; Liu, F. Q.; Harnoode, C. Barbituric Acid-Based Magnetic N-Halamine Nanoparticles as Recyclable Antibacterial Agents. *ACS Appl. Mater. Interfaces* **2013**, *5*, 8125−8133.

(11) Mosaiab, T.; Jeong, C. J.; Shin, G. J.; Choi, K. H.; Lee, S. K.; Lee, I.; In, I.; Park, S. Y. Recyclable and Stable Silver Deposited Magnetic Nanoparticles with Poly (Vinyl Pyrrolidone)-Catechol Coated Iron Oxide for Antimicrobial Activity. *Mater. Sci. Eng., C* **2013**, *33*, 3786−3794.

(12) Dong, H.; Huang, J.; Koepsel, R. R.; Ye, P.; Russell, A. J.; Matyjaszewski, K. Recyclable Antibacterial Magnetic Nanoparticles Grafted with Quaternized Poly (2-(Dimethylamino) Ethyl Methacrylate) Brushes. *Biomacromolecules* **2011**, *12*, 1305−1311.

(13) Liu, Y.; Dong, X.; Chen, P. Biological and Chemical Sensors Based on Graphene Materials. *Chem. Soc. Rev.* **2012**, *41*, 2283−2307.

(14) Hu, W.; Peng, C.; Luo, W.; Lv, M.; Li, X.; Li, D.; Huang, Q.; Fan, C. Graphene-Based Antibacterial Paper. *ACS Nano* **2010**, *4*, 4317−4323.

(15) Tang, J.; Chen, Q.; Xu, L.; Zhang, S.; Feng, L.; Cheng, L.; Xu, H.; Liu, Z.; Peng, R. Graphene Oxide−Silver Nanocomposite as a Highly Effective Antibacterial Agent with Species-Specific Mechanisms. *ACS Appl. Mater. Interfaces* **2013**, *5*, 3867−3874.

(16) Bao, Q.; Zhang, D.; Qi, P. Synthesis and Characterization of Silver Nanoparticle and Graphene Oxide Nanosheet Composites as a Bactericidal Agent for Water Disinfection. *J. Colloid Interface Sci.* **2011**, *360*, 463−470.

(17) Das, M. R.; Sarma, R. K.; Saikia, R.; Kale, V. S.; Shelke, M. V.; Sengupta, P. Synthesis of Silver Nanoparticles in an Aqueous Suspension of Graphene Oxide Sheets and Its Antimicrobial Activity. *Colloids Surf., B* **2011**, *83*, 16−22.

(18) de Faria, A. F.; Mazarin de Moraes, A. C.; Marcato, P. D.; Teodoro Martinez, D. S.; Duran, N.; Souza Filho, A. G.; Brandelli, A.; Alves, O. L. Eco-Friendly Decoration of Graphene Oxide with Biogenic Silver Nanoparticles: Antibacterial and Antibiofilm Activity. *J. Nanopart. Res.* **2014**, 16.

(19) Zhu, Z.; Su, M.; Ma, L.; Ma, L.; Liu, D.; Wang, Z. Preparation of Graphene Oxide-Silver Nanoparticle Nanohybrids with Highly Antibacterial Capability. *Talanta* **2013**, *117*, 449−455.

(20) Li, S.-K.; Yan, Y.-X.; Wang, J.-L.; Yu, S.-H. Bio-Inspired in Situ Growth of Monolayer Silver Nanoparticles on Graphene Oxide Paper as Multifunctional Substrate. *Nanoscale* **2013**, *5*, 12616−12623.

(21) Ocsoy, I.; Paret, M. L.; Ocsoy, M. A.; Kunwar, S.; Chen, T.; You, M.; Tan, W. Nanotechnology in Plant Disease Management: DNA-Directed Silver Nanoparticles on Graphene Oxide as an Antibacterial against Xanthomonas Perforans. *ACS Nano* **2013**, *7*, 8972−8980.

(22) Zhou, Y.; Yang, J.; He, T.; Shi, H.; Cheng, X.; Lu, Y. Highly Stable and Dispersive Silver Nanoparticle-Graphene Composites by a Simple and Low-Energy-Consuming Approach and Their Antimicrobial Activity. *Small* **2013**, *9*, 3445−3454.

(23) He, G. Y.; Wu, H. Q.; Ma, K.; Wang, L.; Sun, X. Q.; Chen, H. Q.; Wang, X. Photosynthesis of Multiple Valence Silver Nanoparticles on Reduced Graphene Oxide Sheets with Enhanced Antibacterial Activity. *Synth. React. Inorg., Met.-Org., Nano-Met. Chem.* **2013**, *43*, 440−445.

(24) Li, C.; Wang, X.; Chen, F.; Zhang, C.; Zhi, X.; Wang, K.; Cui, D. The Antifungal Activity of Graphene Oxide-Silver Nanocomposites. *Biomaterials* **2013**, *34*, 3882−3890.

(25) Cai, X.; Lin, M.; Tan, S.; Mai, W.; Zhang, Y.; Liang, Z.; Lin, Z.; Zhang, X. The Use of Polyethyleneimine-Modified Reduced Graphene Oxide as a Substrate for Silver Nanoparticles to Produce a Material with Lower Cytotoxicity and Long-Term Antibacterial Activity. *Carbon* **2012**, *50*, 3407−3415.

(26) Liu, L.; Liu, J.; Wang, Y.; Yan, X.; Sun, D. D. Facile Synthesis of Monodispersed Silver Nanoparticles on Graphene Oxide Sheets with Enhanced Antibacterial Activity. *New J. Chem.* **2011**, *35*, 1418−1423.

(27) Wu, M.; Lu, D.; Zhao, Y.; Ju, T. Facile Synthesis of Silver-Modified Functionalised Graphene Oxide Nanocomposite with Enhanced Antibacterial Property. *Micro Nano Lett.* **2013**, *8*, 82−85.

(28) Xu, W.-P.; Zhang, L.-C.; Li, J.-P.; Lu, Y.; Li, H.-H.; Ma, Y.-N.; Wang, W.-D.; Yu, S.-H. Facile Synthesis of Silver@Graphene Oxide Nanocomposites and Their Enhanced Antibacterial Properties. *J. Mater. Chem.* **2011**, *21*, 4593−4597.

(29) Zhang, D.; Liu, X.; Wang, X. Green Synthesis of Graphene Oxide Sheets Decorated by Silver Nanoprisms and Their Anti-Bacterial Properties. *J. Inorg. Biochem.* **2011**, *105*, 1181−1186.

(30) Gao, N.; Chen, Y.; Jiang, J. Ag@Fe_2O_3-GO Nanocomposites Prepared by a Phase Transfer Method with Long-Term Antibacterial Property. *ACS Appl. Mater. Interfaces* **2013**, *5*, 11307−14.

(31) Liu, S.; Zeng, T. H.; Hofmann, M.; Burcombe, E.; Wei, J.; Jiang, R.; Kong, J.; Chen, Y. Antibacterial Activity of Graphite, Graphite Oxide, Graphene Oxide, and Reduced Graphene Oxide: Membrane and Oxidative Stress. *ACS Nano* **2011**, *5*, 6971−6980.

(32) Ruiz, O. N.; Fernando, K. S.; Wang, B.; Brown, N. A.; Luo, P. G.; McNamara, N. D.; Vangsness, M.; Sun, Y.-P.; Bunker, C. E. Graphene Oxide: A Nonspecific Enhancer of Cellular Growth. *ACS Nano* **2011**, *5*, 8100−8107.
(33) Tu, Y.; Lv, M.; Xiu, P.; Huynh, T.; Zhang, M.; Castelli, M.; Liu, Z.; Huang, Q.; Fan, C.; Fang, H. Destructive Extraction of Phospholipids from *Escherichia coli* Membranes by Graphene Nanosheets. *Nat. Nanotechnol.* **2013**, *8*, 594−601.
(34) Shin, S. R.; Aghaei-Ghareh-Bolagh, B.; Dang, T. T.; Topkaya, S. N.; Gao, X.; Yang, S. Y.; Jung, S. M.; Oh, J. H.; Dokmeci, M. R.; Tang, X. S. Cell-Laden Microengineered and Mechanically Tunable Hybrid Hydrogels of Gelatin and Graphene Oxide. *Adv. Mater.* **2013**, *25*, 6385−6391.
(35) Shi, X.; Gong, H.; Li, Y.; Wang, C.; Cheng, L.; Liu, Z. Graphene-Based Magnetic Plasmonic Nanocomposite for Dual Bioimaging and Photothermal Therapy. *Biomaterials* **2013**, *34*, 4786−4793.
(36) Yang, K.; Hu, L.; Ma, X.; Ye, S.; Cheng, L.; Shi, X.; Li, C.; Li, Y.; Liu, Z. Multimodal Imaging Guided Photothermal Therapy Using Functionalized Graphene Nanosheets Anchored with Magnetic Nanoparticles. *Adv. Mater.* **2012**, *24*, 1868−1872.
(37) Yang, K.; Zhang, S.; Zhang, G.; Sun, X.; Lee, S.-T.; Liu, Z. Graphene in Mice: Ultrahigh in Vivo Tumor Uptake and Efficient Photothermal Therapy. *Nano Lett.* **2010**, *10*, 3318−3323.
(38) Yang, K.; Feng, L.; Shi, X.; Liu, Z. Nano-Graphene in Biomedicine: Theranostic Applications. *Chem. Soc. Rev.* **2013**, *42*, 530−547.
(39) Ma, X.; Tao, H.; Yang, K.; Feng, L.; Cheng, L.; Shi, X.; Li, Y.; Guo, L.; Liu, Z. A Functionalized Graphene Oxide-Iron Oxide Nanocomposite for Magnetically Targeted Drug Delivery, Photothermal Therapy, and Magnetic Resonance Imaging. *Nano Res.* **2012**, *5*, 199−212.
(40) Chen, Y. W.; Chen, P. J.; Hu, S. H.; Chen, I. W.; Chen, S. Y. Nir-Triggered Synergic Photo-Chemothermal Therapy Delivered by Reduced Graphene Oxide/Carbon/Mesoporous Silica Nanocookies. *Adv. Funct. Mater.* **2014**, *24*, 451−459.
(41) Feng, L.; Wu, L.; Qu, X. New Horizons for Diagnostics and Therapeutic Applications of Graphene and Graphene Oxide. *Adv. Mater.* **2013**, *25*, 168−186.
(42) Shen, H.; Zhang, L.; Liu, M.; Zhang, Z. Biomedical Applications of Graphene. *Theranostics* **2012**, *2*, 283.
(43) Huang, W. C.; Tsai, P. J.; Chen, Y. C. Functional Gold Nanoparticles as Photothermal Agents for Selective-Killing of Pathogenic Bacteria. *Nanomedicine* **2007**, *2*, 777−787.
(44) Ray, P. C.; Khan, S. A.; Singh, A. K.; Senapati, D.; Fan, Z. Nanomaterials for Targeted Detection and Photothermal Killing of Bacteria. *Chem. Soc. Rev.* **2012**, *41*, 3193−3209.
(45) Lin, D.; Qin, T.; Wang, Y.; Sun, X.; Chen, L. Graphene Oxide Wrapped Sers Tags: Multifunctional Platforms toward Optical Labeling, Photothermal Ablation of Bacteria, and the Monitoring of Killing Effect. *ACS Appl. Mater. Interfaces* **2014**, *6*, 1320−1329.
(46) Wu, M.-C.; Deokar, A. R.; Liao, J.-H.; Shih, P.-Y.; Ling, Y.-C. Graphene-Based Photothermal Agent for Rapid and Effective Killing of Bacteria. *ACS Nano* **2013**, *7*, 1281−1290.
(47) Yang, X.; Li, Z.; Ju, E.; Ren, J.; Qu, X. Reduced Graphene Oxide Functionalized with a Luminescent Rare-Earth Complex for the Tracking and Photothermal Killing of Drug-Resistant Bacteria. *Chem.—Eur. J.* **2014**, *20*, 394−398.
(48) Sun, H.; Cao, L.; Lu, L. Magnetite/Reduced Graphene Oxide Nanocomposites: One Step Solvothermal Synthesis and Use as a Novel Platform for Removal of Dye Pollutants. *Nano Res.* **2011**, *4*, 550−562.
(49) Lee, P.; Meisel, D. Adsorption and Surface-Enhanced Raman of Dyes on Silver and Gold Sols. *J. Phys. Chem.* **1982**, *86*, 3391−3395.
(50) Andrews, J. M. Determination of Minimum Inhibitory Concentrations. *J. Antimicrob. Chemother.* **2001**, *48* (Suppl1), 5−16.
(51) Jia, H.; Hou, W.; Wei, L.; Xu, B.; Liu, X. The Structures and Antibacterial Properties of Nano-SiO_2 Supported Silver/Zinc-Silver Materials. *Dent. Mater.* **2008**, *24*, 244−249.
(52) Wang, S. H.; Hou, W. S.; Wei, L. Q.; Jia, H. S.; Liu, X. G.; Xu, B. S. Antibacterial Activity of Nano-SiO_2 Antibacterial Agent Grafted on Wool Surface. *Surf. Coat. Technol.* **2007**, *202*, 460−465.
(53) Zhu, Z. J.; Su, M.; Ma, L.; Liu, D. J.; Wang, Z. X. Preparation of Graphene Oxide-Silver Nanoparticle Nanohybrids with Highly Antibacterial Capability. *Talanta* **2013**, *117*, 449−455.
(54) Feng, Q.; Wu, J.; Chen, G.; Cui, F.; Kim, T.; Kim, J. A Mechanistic Study of the Antibacterial Effect of Silver Ions on *Escherichia coli* and *Staphylococcus aureus*. *J. Biomed. Mater. Res.* **2000**, *52*, 662−668.
(55) Kawahara, K.; Tsuruda, K.; Morishita, M.; Uchida, M. Antibacterial Effect of Silver-Zeolite on Oral Bacteria under Anaerobic Conditions. *Dent. Mater.* **2000**, *16*, 452−455.
(56) Kong, H.; Song, J.; Jang, J. One-Step Fabrication of Magnetic γ-Fe_2O_3/Polyrhodanine Nanoparticles Using in Situ Chemical Oxidation Polymerization and Their Antibacterial Properties. *Chem. Commun.* **2010**, *46*, 6735−6737.